bioRxiv preprint doi: https://doi.org/10.1101/2020.05.25.114991; this version posted June 7, 2021. The copyright holder for this preprint (which was not certified by peer review) is the author/funder, who has granted bioRxiv a license to display the preprint in perpetuity. It is made available under aCC-BY-ND 4.0 International license.

Visual gene expression reveals a cone to rod developmental progression in deep-sea fishes

Nik Lupše[1*], Fabio Cortesi[2], Marko Freese[3], Lasse Marohn[3], Jan-Dag Pohlman[3], Klaus Wysujack[3], Reinhold Hanel[3], Zuzana Musilova[1*]

1) Department of Zoology, Faculty of Science, Charles University, Vinicna 7, 12844 Prague, Czech Republic
2) Queensland Brain Institute, University of Queensland, Brisbane 4072 QLD, Australia
3) Thünen Institute of Fisheries Ecology, Herwigstraße 31, 27572, Bremerhaven, Germany

* corresponding authors; lupsen@natur.cuni.cz, zuzana.musilova@natur.cuni.cz

Keywords: opsin, evolution, mesopelagic, adaptation, convergence, phototransduction, vision, gene expression, rhodopsin

Abstract

Vertebrates generally use cone cells in retina for colour vision and rod cells to see in the dim light. Many deep-sea fishes have only rod cells in the retina, while both rod and cone genes are still preserved in their genomes. As deep-sea fish larvae start their lives in the shallow, well-lit epipelagic zone, they have to cope with diverse environmental conditions during ontogeny. Using a comparative transcriptomic approach in 20 deep-sea fish species from eight teleost orders, we report on a developmental cone-to-rod switch. While adults mostly rely on rod opsin (*RH1*) for vision in the dim light, larvae almost exclusively express mid-wavelength-sensitive cone opsins (*RH2*) in their retinas. The phototransduction cascade genes follow a similar ontogenetic pattern of cone- followed by rod-specific gene expression in most orders, except for the pearleye and sabretooth (Aulopiformes), in which the cone cascade remains dominant throughout development. By inspection of whole genomes of five deep-sea species (four of them sequenced within this study: *Idiacanthus fasciola, Chauliodus sloani*; Stomiiformes; *Coccorella atlantica, Scopelarchus michaelsarsi*; Aulopiformes), we found that deep-sea fish possess mostly the rod RH1 opsin, and multiple copies of the green-sensitive RH2 opsin genes in their genomes, while other cone opsin classes have been lost. Our findings provide molecular support for a limited opsin gene repertoire and a conserved vertebrate pattern whereby cone

bioRxiv preprint doi: https://doi.org/10.1101/2020.05.25.114991; this version posted June 7, 2021. The copyright holder for this preprint (which was not certified by peer review) is the author/funder, who has granted bioRxiv a license to display the preprint in perpetuity. It is made available under aCC-BY-ND 4.0 International license.

34 photoreceptors develop first and rod photoreceptors are added only at later developmental
35 stages.

bioRxiv preprint doi: https://doi.org/10.1101/2020.05.25.114991; this version posted June 7, 2021. The copyright holder for this preprint (which was not certified by peer review) is the author/funder, who has granted bioRxiv a license to display the preprint in perpetuity. It is made available under aCC-BY-ND 4.0 International license.

INTRODUCTION

Vision is a primary sense used by most vertebrates for navigation, predator avoidance, communication and to find food and shelter. At its initiation, vertebrate vision is enabled by cone (photopic, colour vision) and rod (scotopic, mostly colour blind) photoreceptors in the retina containing a light absorbing pigment that consists of an opsin protein covalently bound to a vitamin-A-derived chromophore (Lamb 2013). The absorbance of photons by the chromophore leads to a conformational change of the opsin protein, which initiates a photoreceptor-specific G-protein-coupled phototransduction cascade, propagating the signal to the brain (Downes & Gautam 1999, Larhammar et al. 2009, Lamb et al. 2019). It is thought that the development of the visual system follows a conserved molecular pattern whereby cone specific genes are activated first before the rod molecular pathway is initiated later during ontogeny (Mears et al. 2001, Shen & Raymond 2004, Sernagor et al. 2006). However, whether this is the case for all vertebrates and especially for those that have retinas that contain only rods as adults, remains unclear.

Changes in the light environment, ecology, and phylogenetic inertia are thought to be primary drivers for visual system diversity in vertebrates (Hunt et al. 2014). For example, most mesopelagic deep-sea fishes (200 – 1,000 m depth), either living strictly at depth or migrating to the shallows at night, have evolved visual systems that are sensitive to the dominant blue light (~ 470 – 490 nm) of their environment (Turner et al. 2009). Moreover, as the daylight and the bioluminescent light emitted by deep-sea critters are quickly dimmed with depth, deep-sea fish visual systems have evolved peculiar morphologies to maximise photon capture including barrel-eyes, reflective tapeta and the use of rod-dominated and in many cases rod-only retinas that might be stacked into multiple banks (reviewed in de Busserolles et al. 2020). However, most mesopelagic fishes start their lives in the shallow well-lit epipelagic zone (0 – 200 m depth) (Moser & Smith 1993, Sassa & Hirota 2013). Consequently, their visual systems must cope with a variety of light intensities and spectra throughout development.

Studies investigating the gene expression in the retina of deep-sea fishes are scarce and usually focus on a selected few species (Zhang et al. 2000, Douglas et al. 2016; de Busserolles et al. 2017, Musilova et al. 2019a, Byun et al. 2020). In adults, species with pure rod retinas tend to only express rod opsin(s) (Douglas et al. 2016, Musilova et al. 2019a), albeit two species of pearlsides (*Maurolicus* spp.) have been found to express cone-specific genes (i.e., cone transduction pathway and opsin genes) inside rod-looking cells (de Busserolles et al. 2017). It remains unknown whether deep-sea fishes that have a low proportion of cone photoreceptors as adults (e.g. Munk 1990, Collin et al. 1998, Bozanno et al. 2007, Pointer et al. 2007, Biagioni

bioRxiv preprint doi: https://doi.org/10.1101/2020.05.25.114991; this version posted June 7, 2021. The copyright holder for this preprint (which was not certified by peer review) is the author/funder, who has granted bioRxiv a license to display the preprint in perpetuity. It is made available under aCC-BY-ND 4.0 International license.

et al. 2016) also express cone-specific genes at any stages of their lives or whether molecularly these fishes rely on the rod machinery alone. To investigate whether the retinal development in deep-sea fishes follows a similar cone-to-rod molecular pathway as found in other vertebrates or whether some species start their lives with rod pathway activated, we set out to sequence the retinal transcriptomes of 20 deep-sea fish species, including the larval stages in ten species, belonging to eight different teleost orders (Argentiniformes, Aulopiformes, Beryciformes, Myctophiformes, Pempheriformes, Scombriformes, Stomiiformes and Trachichthyiformes). We have further investigated the genomic repertoire in five selected species.

RESULTS AND DISCUSSION

Opsin gene repertoire in the genome. In teleost fishes, gene duplications and deletions followed by functional diversification have resulted in extant species having between 1-40 visual opsin genes within their genomes (Musilova et al., 2019a; Musilova et al., 2021). These genes are defined by their phylogeny and their spectrum of maximal sensitivity (λ_{max}) and fall within five major classes, four cone opsins ('ultraviolet or UV sensitive' *SWS1*: 347–383 nm, 'blue' *SWS2*: 397–482 nm, 'green' *RH2*: 452–537 nm and 'red' *LWS*: 501–573 nm) and one rod opsin ('blue-green' rhodopsin, *RH1* or Rho: 447–525 nm) (Carleton et al. 2020). We analyzed whole genomes of five deep-sea species (sawtail fish *Idiacanthus fasciola*, viperfish *Chauliodus sloani*; both Stomiiformes; sabretooth *Coccorella atlantica*, pearleye *Scopelarchus michaelsarsi*; both Aulopiformes; and fangtooth *Anoplogaster cornuta*,; Trachichthyiformes). All species possess one or two copies of the rod opsin *RH1* gene, and one to seven copies of the *RH2* cone opsin (Fig. 1). All other cone opsin classes, i.e. the *SWS1*, *SWS2* (except for the fangtooth) and *LWS* are missing and have been putatively lost in evolution. This is in accord with the observation that the *LWS* gene abundance decreases with the habitat depth (Musilova et al., 2019a). Such limited genomic repertoire most likely represents an evolutionary response to the deep-sea scotopic environment where also the shortest (UV-violet) and longest (red) wavelengths of light get filtered out first in the water column (reviewed in Musilova et al., 2021, De Busserolles et al., 2020, and Carleton et al., 2020). The increased RH2 diversity observed in the two aulopiform species, on the other hand, illustrates the versatility of this cone opsin class and confirms its dominance in various dimmer-light habitats (Musilova & Cortesi, 2021). Here we confirm that *RH2* is undoubtedly the most important (and often the only) cone opsin gene present in deep-sea fish genomes.

bioRxiv preprint doi: https://doi.org/10.1101/2020.05.25.114991; this version posted June 7, 2021. The copyright holder for this preprint (which was not certified by peer review) is the author/funder, who has granted bioRxiv a license to display the preprint in perpetuity. It is made available under aCC-BY-ND 4.0 International license.

Visual opsin gene expression. Transcriptomic sequencing of 20 deep-sea teleost species revealed that deep-sea fishes mainly express rod opsins and/or green-sensitive cone opsins (*RH2*s) in their retinas (Fig. 1, Table 1). While larvae mostly expressed *RH2*, adults and juveniles mostly expressed *RH1* and in a few cases a combination of both. We found none or very low expression of any of the other cone opsin genes: the red sensitive *LWS* was not expressed at all, the UV sensitive *SWS1* was only found in the larva of the whalefish, *Gyrinomimus* sp. (Beryciformes), and the blue/violet sensitive *SWS2* only in the larvae of the whalefish, and the fangtooth, *Anoplogaster cornuta* (Trachichthyiformes), (Fig. 1, Table 1). Differences in gene expression patterns are likely to be driven by ontogenetic transitions in light habitat from bright to dim environments and also by changes in ecological demands, as discussed in more detail below.

Similar to the opsin genes, we also detected ontogenetic differences in the expression of phototransduction cascade genes (Fig. 2). Here we focused on the comparison of five species from three teleost orders for which we had both larval and adult specimens available and found that the cone-specific genes were mostly expressed in the larval stages (e.g., cone transducin, *GNAT2*), while adults from three species mostly expressed rod-specific genes (e.g., rod transducin, *GNAT1*; Fig. 2b). Hence, at the molecular level, the visual systems of deep-sea fishes start out with a cone-based expression pattern. Moreover, in the fangtooth, where samples from various sized specimens were available, we found that the cone-specific expression was gradually replaced with the rod profile as the fish grew (Fig. 2c, Table S1). This is similar to the visual development in shallower living fishes (e.g., Atlantic cod (Valen et al. 2016), zebrafish (Sernagor et al. 2006)) and terrestrial vertebrates (e.g., mice (Mears et al. 2001), rhesus monkey (La Vail et al. 1991)), where cone photoreceptors are first to develop, followed by temporally and spatially distinct rods (Raymond 1995, Shen & Raymond 2004). The cone-to-rod developmental sequence is therefore likely to be shared across vertebrates, even in species that have pure rod retinas as adults.

Ontogenetic shift in expression profiles and the transition phase. The developmental changes in the visual system we uncovered are best explained by the different habitats larval and adult deep-sea fishes inhabit. In general, deep-sea fish larvae live in the shallow epipelagic zone (Moser & Smith 1993) where ambient light levels are sufficiently high to warrant a cone-based visual system. After metamorphosis, deep-sea fishes start to submerge deeper and take up a life at different depths in the mesopelagic or even bathypelagic (below 1,000 m depth) zone, where the sun- and moonlight is gradually replaced by bioluminescence as the main

bioRxiv preprint doi: https://doi.org/10.1101/2020.05.25.114991; this version posted June 7, 2021. The copyright holder for this preprint (which was not certified by peer review) is the author/funder, who has granted bioRxiv a license to display the preprint in perpetuity. It is made available under aCC-BY-ND 4.0 International license.

source of light (Denton 1990). In this extremely dim environment, rods work at their best and cone photoreceptors would be obsolete for the most part at least. Rod-based vision is also favoured in those deep-sea species that exhibit diel vertical migrations to feed in the plankton rich surface layers at night (de Busserolles et al. 2020). In addition, we discovered that in some species there was a switch in the type of cone-based *RH2* opsin that was expressed (Fig. 1). For example, in Aulopiformes, the larvae expressed an RH2 that is presumably sensitive to longer wavelengths of light compared to the RH2 that was found in adults (Table 2). This clearly shows that larval and adult deep-sea fishes rely on different opsin expression profiles, which is similar to ontogenetic changes in opsin gene expression in diurnal shallow-water fishes such as freshwater cichlids (Carleton et al. 2016) and coral reef dottybacks (Cortesi et al. 2015, 2016) or between the freshwater and deep-sea maturation stages in eels (Zhang et al., 2000).

Our data furthermore suggests that the ontogenetic change in visual gene expression precedes morphological changes such as metamorphosis from larva to juvenile and also habitat transitions. For example, in the fangtooth, the larvae which were collected from the shallows (0 – 300 m) showed increasing amounts of *RH1* expression with growth, despite displaying larval phenotypes throughout (horns and small teeth; Fig. 1). A similar pattern of changing opsin gene expression ahead of metamorphosis has also been reported from shallow-water fishes such as European eels (Bowmaker et al. 2008), dottybacks (Cortesi et al. 2016) and surgeonfishes (Tettamanti et al. 2019). Interestingly, all our fangtooth larvae (incl. the smallest individual with a total length of 4 mm) already expressed a small amount of *RH1* (Fig. 2c). Whether fangtooth start their lives with a pure-cone retina or low-levels of rod opsin expression are normal even in pre-flexation larvae remains therefore unclear. In addition to the green-sensitive cone opsin *RH2*, the fangtooth larvae also expressed low levels of the blue-sensitive *SWS2*, potentially conferring dichromatic colour vision to the early life stages of this species (Fig. 1).

Photoreceptor cell identities. Interestingly, two aulopiform species; the Atlantic sabretooth, *Coccorella atlantica*, and the Bigfin pearleye, *Scopelarchus michaelsarsi*, despite expressing mostly *RH1* as adults, retained a cone-dominated phototransduction cascade expression profile akin to the one found in the larval stages (Fig. 2, Table S1). This begs the question whether the photoreceptors they are using are of cone or rod nature. Initially described in snakes and geckos (Simoes et al. 2016, Schott et al. 2019) and recently also in a deep-sea fish (de Busserolles et al. 2017), it appears that the dichotomy of rods and cones is not always as clear cut as one

bioRxiv preprint doi: https://doi.org/10.1101/2020.05.25.114991; this version posted June 7, 2021. The copyright holder for this preprint (which was not certified by peer review) is the author/funder, who has granted bioRxiv a license to display the preprint in perpetuity. It is made available under aCC-BY-ND 4.0 International license.

might think. For example, adult deep-sea pearlsides, *Maurolicus* spp. have a retina that expresses ~ 99% *RH2* and ~ 1% *RH1* with corresponding cone and rod phototransduction gene expressions. Their photoreceptors, however, are all rod-shaped and careful histological examination has shown that these consist of a tiny proportion of true rods and a majority of transmuted rod-like cones (de Busserolles et al. 2017). In the case of the pearlside, and also in geckos and snakes, the opsin and phototransduction genes correspond to each other making it possible to distinguish photoreceptor types at the molecular level. However, in the aulopiforms, high expression of rod opsin is seemingly mismatched with high levels of cone phototransduction gene expression (Fig. 2). In salamanders, the opposite pattern can be found whereby a cone opsin is combined with the rod phototransduction cascade inside a rod looking cone photoreceptor (Mariani 1986). Anatomically, the retina of *S. michaelsarsi* is composed of mostly rods with low numbers of cone cells (Collin et al. 1998), while the adult retina of *Evermanella balbo,* an evermannellid species related to *C. atlantica,* appears to consist of two differently looking rod populations (Wagner et al. 2019). It is therefore likely, that similar to what was found in pearlsides (de Busserolles et al. 2017), these fishes have a high proportion of transmuted rod-like cone photoreceptors that use *RH1* instead of a cone opsin as the visual pigment. Alternatively, a proportion of true rods might make use of the cone phototransduction cascade. Either way, combining more stable rod opsin in a rod-shaped cell with the cone-specific cascade is likely to increase sensitivity while also maintaining high transduction and recovery speeds of cells (Baylor 1987, Kawamura & Tachibanaki 2012, Luo et al. 2020). Histology, fluorescent in-situ hybridisation and ideally physiological recordings are needed to ultimately disentangle the identity of photoreceptor cells in aulopiform.

Evolutionary history of deep-sea fish opsins. While the majority of adult fishes relied on a single *RH1* copy, three species were found that expressed multiple *RH1* copies: The Warming's lanternfish, *Ceratoscopelus warmingii* (Myctophiformes), expressed three different *RH1* genes, and *S. michaelsarsi* and the basslet, *Howella brodiei* (Pempheriformes), expressed two copies each. Larvae and a few adult deep-sea fishes mostly expressed a single *RH2* copy, except for the pearleyes, *Scopelarchus* spp., and the Reinhardt's lanternfish, *Hygophum reinhardtii*, which expressed three larval copies each, and the whalefish which expressed five larval copies (Fig. 1).

The *RH1* and *RH2* phylogenies revealed that most deep-sea fish visual opsins cluster together by species or order (Fig. 3). For example, in the whalefish all *RH2s* are clustered together suggesting that these genes are lineage or species-specific (Fig. 3b). However, there

bioRxiv preprint doi: https://doi.org/10.1101/2020.05.25.114991; this version posted June 7, 2021. The copyright holder for this preprint (which was not certified by peer review) is the author/funder, who has granted bioRxiv a license to display the preprint in perpetuity. It is made available under aCC-BY-ND 4.0 International license.

were a few exceptions, suggesting more ancient duplication events. In *Scopelarchus* the two *RH1* copies are not in a sister relationship and result in different clusters, suggesting that these copies originated in the common ancestor of aulopiforms or perhaps even earlier (Fig. 3a). Also, the *RH2s* in aulopiforms (*Scopelarchus*, *Coccorella*) cluster by ontogenetic stage, making it likely that the developmental switch in gene expression was already present in the aulopiform ancestor (Fig. 3b).

Molecular complexity of deep-sea fish visual systems. The complexity of deep-sea fish visual systems at the molecular level varied quite substantially. For example, the three Stomiiformes species: The Ribbon sawtail fish, *Idiacanthus fasciola*, and two species of viperfish, *Chauliodus sloani* and *Ch. danae*, appeared to have a very basic visual set up; these fishes were found to express a single *RH2* cone opsin and a single *RH1* rod opsin as larvae and adults, respectively (Fig. 1). On the contrary, a number of the deep-sea fish orders examined here expressed more than two opsin genes. Adult lanternfishes and basslets have rod-only retinas but expressed multiple *RH1* copies that have functionally diversified (Fig. 3). Other species expressed both cone and rod opsins as adults (some aulopiform species and *Scombrolabrax*), which is similar to the opsin gene expression profiles found in shallow-living nocturnal reef fishes (Cortesi et al. 2020).

The most complex visual system described here was found in *S. michaelsarsi*. In general, this species is known for its numerous morphological and anatomical adaptations to vision in the deep-sea, including having barrel eyes with a main and an accessory retina, rods that are organised in bundles, large ganglion cells and corneal lens pads (Collin et al., 1998). The two copies of *RH1* (*RH1a* and *RH1b*) it expressed showed high sequence diversity differing in 66 amino acids, three of which are key tuning sites likely to change the spectral sensitivity of the pigments via a shift in λ_{max} (Fig. 3, Tables 2 and 3) (Yokoyama 2008, Musilova et al. 2019a, Yokoyama & Yia 2020). This supports the findings by Pointer et al. (2007) (Pointer et al. 2007) which using microscpetrophotometry (MSP) in another pearleye species, *S. analis*, found two rod photoreceptors with different absorption maxima at 479 and 486 nm. The situation is less clear for the green-sensitive *RH2* opsin. While in *S. analis* cones have been found in the accessory and main retinas, in *S. michaelsarsi* cone photoreceptors appear restricted to the accessory retina alone (Collin et al. 1998). This is intriguing as it suggests substantial differences in visual systems even between closely related species from the same genus.

bioRxiv preprint doi: https://doi.org/10.1101/2020.05.25.114991; this version posted June 7, 2021. The copyright holder for this preprint (which was not certified by peer review) is the author/funder, who has granted bioRxiv a license to display the preprint in perpetuity. It is made available under aCC-BY-ND 4.0 International license.

The visual ecology of deep-sea fishes. We found molecular support for deep-sea visual adaptations on multiple levels:

1) Opsin gene diversity in the genome. Retinal transcriptomes in the Stomiiformes pointed towards a simple visual system that expresses a single opsin gene at different developmental stages (*RH2* in larvae, *RH1* in adults) (Fig. 1). Besides RH2, searching for visual opsins in a newly sequenced (*I. fasciola* and *Ch. sloani*) and several published genomes (Musilova et al., 2019a), revealed that Stomiiformes are likely to have lost all other cone opsin gene families (Fig. 1). For *RH2*, they seem to only have a single or at most two gene copies, which is substantially less compared to other teleosts (Musilova et al. 2019a). The Stomiiform example, therefore, shows that a decrease in light intensity and the spectrum of light in the deep-sea may not only restrict gene expression at adult stages, but also lead to the loss of opsin genes altogether. Similarly, a loss in opsin and other vision-related genes (e.g. otx5b, crx) has previously been reported from shallow living fishes that are either nocturnal (Luehrmann et al. 2019), live in murky waters (Liu et al. 2019), or inhabit caves or similarly dim environments (Huang et al. 2019, Musilova et al. 2019a).

2) Visual gene expression. Previous work has found that the expression of the longest- (*LWS* - red) and shortest- (*SWS1* - UV) sensitive opsins is reduced or absent in deeper living coral reef fishes (Cortesi et al. 2020) and also in fishes inhabiting deep freshwater lakes (e.g., Hunt 1997, Sugawara et al. 2005, Musilova et al. 2019b), which is correlated with a loss of short- and long-wavelengths with depth. Accordingly, we found here that deep-sea fishes lack any *LWS* expression even in the shallow-living larval stages (Fig. 1), which is accompanied by the loss of *LWS* cone opsin in many deep-sea fish lineages (Musilova et al. 2019a). Similarly, *SWS1* is not expressed in any of the species studied, except for in the larval whalefish, and is also absent from many deep-sea fish genomes (Fig. 1) (Musilova et al. 2019a). However, shallow larval stages are likely to explain why all deep-sea fishes studied to date maintain at least some cone opsins in their genomes (Musilova et al. 2019a).

Most deep-sea fish larvae expressed a single *RH2* gene, but the larvae of some species (fangtooth, whalefish and lanternfish) expressed multiple cone opsin genes, likely providing them with similar visual systems to the larvae of shallow-living marine (Britt et al. 2001) and freshwater species (Carleton et al. 2016), possibly aiding them in detecting residual light, discriminating brightness and/or colours. Juvenile deep-sea fishes, on the other hand, showed rod-based expression profiles also found in the adult stages (Fig. 1). This shift in opsin gene expression correlates with developmental changes in ecology. As opposed to the adults which

bioRxiv preprint doi: https://doi.org/10.1101/2020.05.25.114991; this version posted June 7, 2021. The copyright holder for this preprint (which was not certified by peer review) is the author/funder, who has granted bioRxiv a license to display the preprint in perpetuity. It is made available under aCC-BY-ND 4.0 International license.

are exposed to a narrow and dim light environment where food is scarce, larvae typically live in well-lit, broad spectrum shallow waters where food and predators are abundant (Moser & Smith 1993).

3) Functional adaptation in key spectral tuning sites. When multiple *RH1* copies were expressed, they often showed distinct differences in key amino acid sites that are likely to shift the spectral sensitivities of the pigments (Fig. 3 and Tables 2 and 3) (Yokoyama 2008, Musilova et al. 2019a). As such, the three different *RH1*s in *C. warmingii* differed in 15 key-tuning sites. Opsin gene expression together with spectral-sensitivity estimations revealed a dominant rod opsin copy (*RH1-1*), and a shorter- (*RH1-2*) and a longer-shifted (*RH1-3*) copy with lower transcript levels (Figs. 1 and 3). The MSP in *C. warmingii* found two distinct rod types with λ_{max} values of 488 and 468 nm (Collin and Marshall 2003) corresponding most likely to the RH1a and RH1b, respectively. It is possible that multiple *RH1* copies are coexpressed within the same photoreceptor, something that has previously been reported for cone opsins in shallow-water marine (Savelli et al. 2018, Stieb et al. 2019) and freshwater fishes (Dalton et al. 2014, Torres-Dowdall et al. 2017). Coexpression could produce visual pigment mixtures that shift photoreceptor sensitivity and enhance visual contrast, aiding in predator-prey interactions or mate finding (Dalton et al. 2014). Alternatively, a third rod photoreceptor type might have been overlooked during MSP, which can occur especially if the cell-type is rare. While the function of having multiple rod opsins in *C. warmingii* remains to be investigated, several possible benefits for a multi-rod visual system have recently been proposed including that it might enable conventional or unusual colour vision in dim light, it might be used to increase visual sensitivity, or enhance object's contrast against a certain background (Musilova et al. 2019a).

In *H. brodiei*, the second *RH1* copy (*RH1-2*) differed in two key tuning sites, E122Q (-15 nm) and G124S (-11 nm), known to cause major short-wavelength shifts in other fishes (Yokoyama 2008). This supports the MSP measurements in its sister species, *Howella sherborni*, which found two different rod types with spectral sensitivities of 463 and 492 nm (Fig. 2) (Partridge et al. 1989).

Having multiple differently tuned rod photoreceptors, one centred on the prevailing light (bioluminescence and/or ambient light ~ 480 – 490 nm) and a second one that is offset from it (i.e. the offset pigment hypothesis; Lythgoe 1966), may be beneficial to break counter illumination - a way of active camouflage in mesopelagic organisms where ventral photophores emit bioluminescent light that matches the residual down-welling light (Denton et all. 1985).

bioRxiv preprint doi: https://doi.org/10.1101/2020.05.25.114991; this version posted June 7, 2021. The copyright holder for this preprint (which was not certified by peer review) is the author/funder, who has granted bioRxiv a license to display the preprint in perpetuity. It is made available under aCC-BY-ND 4.0 International license.

Hence, revealing an individual's silhouette could help to distinguish prey and predators from the background lighting, or visually finding mates. Apart of lanternfishes with three (or more) and basslets with two rod opsins, or exceptional cases of tube-eye (six) and spinyfin (38), the majority of the deep-sea fishes however seems to have only one rod opsin (Musilova et al., 2019a).

Conclusions

So far, the development of deep-sea fish vision at the molecular level had not been studied and only limited morphological information was available. In this study we compared opsin and visual gene expression between 20 deep-sea fish species revealing a major change in expression between larval and adult stages. While deep-sea fish genomes contain both cone and rod opsin genes, larvae rely on the cone pathway and most adult fishes switch to a rod-dominated or rod-only visual system. The cone vs. rod-specific phototransduction cascade genes follow the opsins in some lineages, however, not in aulopiforms. We detected limited opsin gene repertoire in the genomes of five deep-sea fish species composed only of one rod (RH1) and one or two cone (RH2, SWS2) opsin gene classes. Interestingly, we have discovered lineage-specific opsin gene duplications, possibly allowing for increased visual sensitivity and certain kind of colour vision in the depth in some species. Our molecular results therefore support a conserved developmental progression in vertebrates whereby cones appear first in the retina and rod photoreceptors are added later during development.

bioRxiv preprint doi: https://doi.org/10.1101/2020.05.25.114991; this version posted June 7, 2021. The copyright holder for this preprint (which was not certified by peer review) is the author/funder, who has granted bioRxiv a license to display the preprint in perpetuity. It is made available under aCC-BY-ND 4.0 International license.

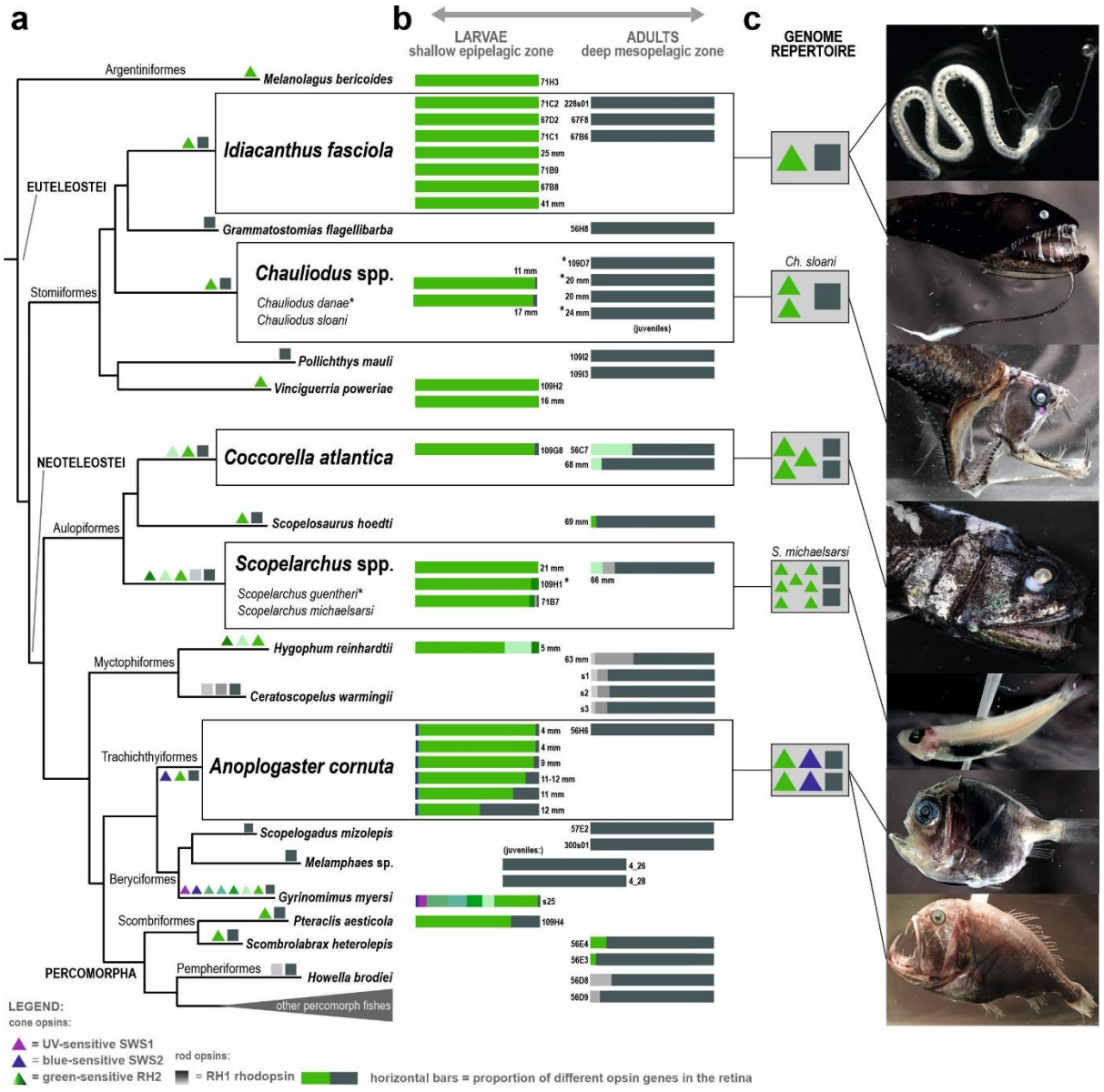

Fig. 1: Cone and rod opsin gene expression in larval and adult deep-sea fishes*. A) Transcriptomes were used to characterise the opsin gene expression in the retinas of 20 deep-sea fish species, belonging to eight different orders and mapped onto a simplified teleost phylogeny (topology after Betancur et al., 2017). Boxes highlight the five species for which both larval and adult samples were available. B) Proportional opsin gene expression for each individual (horizontal bar) at different developmental stages. Different colours correspond to cone (colours) or rod (shades of grey) opsin genes, depicted as the proportional expression over the total sum of visual opsins expressed. Different shades of the same colour represent multiple copies of the same gene family. Based on the opsin gene expression, the larvae (left column) show a pure-cone or cone-dominated retina, while the adults (right column) have a pure-rod or rod-dominated visual system. Juvenile specimens in two species had an adult expression profile. Note that some species expressed multiple RH1 copies (*Scopelarchus, Howella brodiei *and* Ceratoscopelus warmingii *adults) or multiple RH2 copies (*Gyrinomimus *sp. larva,* Hygophum reinhardtii *larva). Notably, adults and larvae of* Scopelarchus *sp. and* Coccorella atlantica *expressed different copies of RH2 (more details in Fig. 2). Details about the samples and expression levels are listed in Table 1. C) The genomic repertoire*

bioRxiv preprint doi: https://doi.org/10.1101/2020.05.25.114991; this version posted June 7, 2021. The copyright holder for this preprint (which was not certified by peer review) is the author/funder, who has granted bioRxiv a license to display the preprint in perpetuity. It is made available under aCC-BY-ND 4.0 International license.

342 *of the visual opsins is shown for five species* Idiacanthus fasciola, Chauliodus sloani, Coccorella atlantica,
343 Scopelarchus michaelsarsi *(all this study), and* Anoplogaster cornuta *(Musilova et al., 2019a). The rod RH1 opsin*
344 *and the cone RH2 opsin genes are present in all studied species in one or multiple (up to seven) copies. The SWS2*
345 *opsin gene was found only in the fangtooth, and the SWS1 and LWS are missing from all five studied genomes.*
346

bioRxiv preprint doi: https://doi.org/10.1101/2020.05.25.114991; this version posted June 7, 2021. The copyright holder for this preprint (which was not certified by peer review) is the author/funder, who has granted bioRxiv a license to display the preprint in perpetuity. It is made available under aCC-BY-ND 4.0 International license.

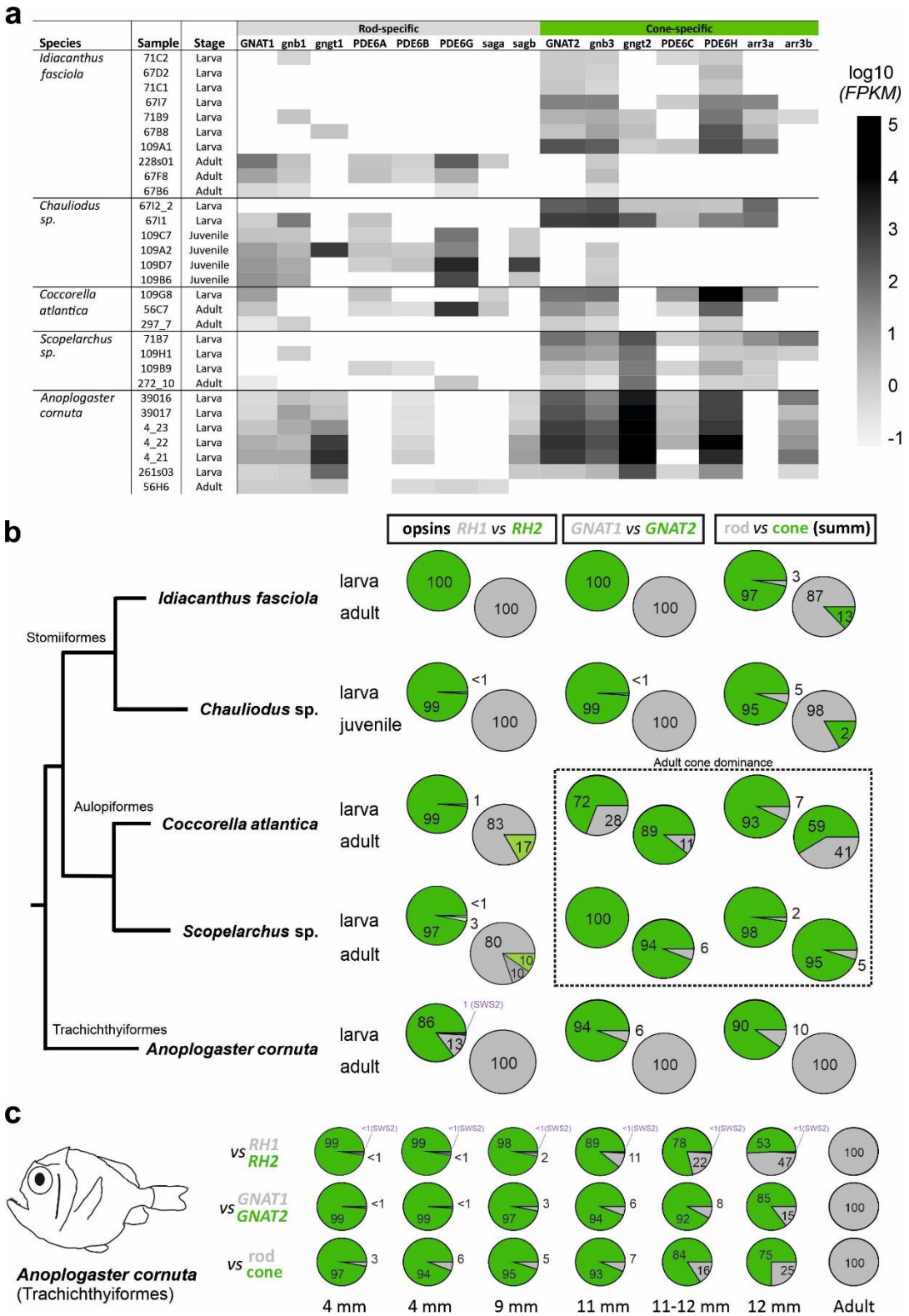

Fig. 2: *Phototransduction cascade gene expression in the retina of five deep-sea fish species. A) Heat map of the expression of individual phototransduction cascade genes for each sample, based on normalised numbers of reads (FPKM). B) Pie charts comparing mean values of relative expression of the opsin genes (rod RH1 and cone RH2), photoreceptor-specific cascade transducin genes (rod-type GNAT1 and cone-type GNAT2), and all cascade genes (photoreceptor-specific transducins, arrestins and phosphodiesterases) summarized. The black square highlights*

bioRxiv preprint doi: https://doi.org/10.1101/2020.05.25.114991; this version posted June 7, 2021. The copyright holder for this preprint (which was not certified by peer review) is the author/funder, who has granted bioRxiv a license to display the preprint in perpetuity. It is made available under aCC-BY-ND 4.0 International license.

354 *the two aulopiform species with the discordance between the opsin type (rod-specific) and phototransduction*
355 *cascade genes (cone-specific) in adults. C) Focus on the common fangtooth (*Anoplogaster cornuta*) transitional*
356 *phase shown as a sequence for six larval and one adult sample; size given as standard length (SL). Note that all*
357 *fangtooth larvae expressed both RH1 and RH2, with an increasing proportion of RH1 to RH2 as the larvae*
358 *increased in size. These individuals all had traits of larval phenotypes (dorsal and ventral horns and small teeth;*
359 *Fig. 1) and were collected relatively shallow between 0-300 m using the plankton trawls.*
360

bioRxiv preprint doi: https://doi.org/10.1101/2020.05.25.114991; this version posted June 7, 2021. The copyright holder for this preprint (which was not certified by peer review) is the author/funder, who has granted bioRxiv a license to display the preprint in perpetuity. It is made available under aCC-BY-ND 4.0 International license.

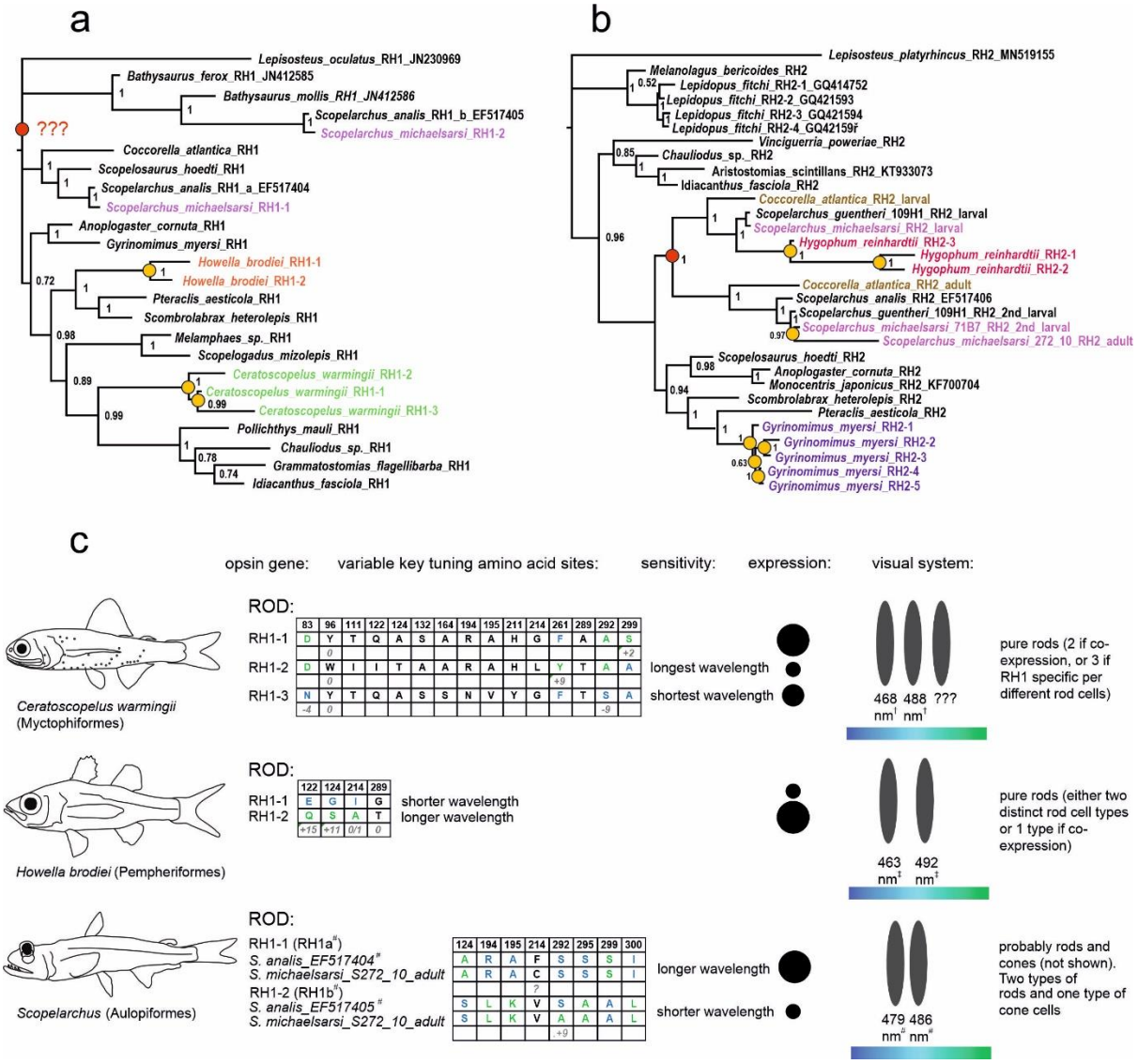

Fig. 3*: Gene trees of the A) RH1 and B) RH2 opsin genes mined from the retinal transcriptomes of deep-sea fishes. Species with multiple copies are highlighted in colour. Additional gene sequences from public databases are listed with their GenBank accession numbers. Note the topology within Aulopiformes; the adult RH2s of* Cocorrella atlantica *and* Scopelarchus *cluster together as do the major larval RH2s. Circles mark gene duplication events with red circles pinpointing (A) the ancestral duplication of RH1 impacting the* Scopelarchus *genus, and (B) the duplication of RH2 in the aulopiform ancestor (or at least the common ancestor of* Coccorella and Scopelarchus). *C) Predicted rod photoreceptor spectral sensitivities based on key spectral tuning site mutations in species with multiple rod opsins. Multiple rod opsins differed in three species,* Ceratoscopelus warmingii *(Myctophiformes),* Howella brodiei *(Pempheriformes) and* Scopelarchus michaelsarsi *(Aulopiformes),*

bioRxiv preprint doi: https://doi.org/10.1101/2020.05.25.114991; this version posted June 7, 2021. The copyright holder for this preprint (which was not certified by peer review) is the author/funder, who has granted bioRxiv a license to display the preprint in perpetuity. It is made available under aCC-BY-ND 4.0 International license.

MATERIALS AND METHODS

Specimens used in this study were collected in the Sargasso Sea during two multipurpose fishery surveys conducted by the German Thünen Institute of Fisheries Ecology onboard the research vessel *Walther Herwig III* in March to April in 2014 and in 2017. The sampling of adults occurred during both day and night at depths of 600 – 1'000 m using a mid-water pelagic trawl net (Engel Netze, Bremerhaven, Germany) with an opening of 30 m x 20 m, a length of 145 m, and mesh sizes (knot to knot) from 90 cm decreasing stepwise to 40, 20, 10, 5, 4, 3, 2 cm, with a 1.5-cm mesh in the 27-m-long codend. The larvae were mostly collected using an Isaacs-Kidd Midwater Trawl net (IKMT; 6.2 m^2 mouth-opening, 0.5 mm mesh size; Hydro-Bios Apparatebau GmbH) at depths of 0 - 300 m by double-oblique transect tows. Adult fish were flash-frozen at -80 ^{0}C upon arrival on board and their fin clip was stored in 96% ethanol. Larval samples were fixed in RNAlater^{TM} (ThermoFisher) and stored at -80 ^{0}C until further use.

To sequence the whole genome of *Idiacanthus fasciola, Chauliodus sloani, Coccorella atlantica,* and *Scopelarchus michaelsarsi,* the genomic DNA was extracted from the fin clip using the DNeasy Blood and Tissue kit (Qiagen) following the enclosed protocol. The library preparation and genome sequencing on Illumina NovaSeq platform (150 bp PE and the yield over 20 Gb per genome) has been outsourced to the sequencing centre Novogene, Singapore (https://en.novogene.com/). To analyze the opsin gene repertoire, the raw genomic reads were mapped in Geneious software version 11.0.3 (Kearse et al. 2012) against the opsin references (single exons of all five opsin classes from the reference species: Nile tilapia, Round goby, Blind cavefish, Spotted gar), as well as against the genes found in the transcriptomes of each species. The parameters have been set to the Medium Sensitivity to capture all reads that match any visual opsin gene. The captured reads mapping to all exons were then remapped against one reference per exon and the species-specific consensus sequence has been generated. If present, multiple paralogous genes were disentangled manually and the consensus sequence has been exported for each variant (see below more details for the transcriptomic analysis). The obtained consensus sequences served as references for the second round of mapping, when all genomic reads were again mapped with the Low Sensitivity settings, and each reference has been then elongated by the overhanging sequence. This step has been repeated until the full gene region has been covered. In case of *Scopelarchus michaelsarsi,* we were not able to cover the full length of five out of seven RH2 genes and these are reported in two parts, one covering the exon 1 and 2, and one covering exons 3, 4 and 5. All genomic data are available in the

bioRxiv preprint doi: https://doi.org/10.1101/2020.05.25.114991; this version posted June 7, 2021. The copyright holder for this preprint (which was not certified by peer review) is the author/funder, who has granted bioRxiv a license to display the preprint in perpetuity. It is made available under aCC-BY-ND 4.0 International license.

406 GenBank database (acc. no *tba*) and the opsin gene sequences are provided as Supplementary
407 file 1.
408
409 Total RNA was extracted from the whole eyes using either the RNeasy micro or mini kit
410 (Qiagen) and the extracted RNA concentration and integrity were subsequently verified on a
411 2100 Bioanalyzer (Agilent). RNAseq libraries for 31 samples were constructed in-house from
412 unfragmented total RNA using Illumina's NEBNext Ultra II Directional RNA library
413 preparation kit, NEBNext Multiplex Oligos and the NEBNext Poly(A) mRNA Magnetic
414 Isolation Module (New England Biolabs). Multiplexed libraries were sequenced on the
415 Illumina HiSeq 2500 platform as 150 bp paired-end (PE) reads. Library construction and
416 sequencing (150 bp PE) for an additional 10 samples was outsourced to Novogene, Singapore
417 (https://en.novogene.com/). We additionally re-analyzed 11 retinal transcriptomes previously
418 published in Musilová et al. (2019a). Together, then, our dataset comprised 52 samples of
419 which, based on morphology, 25 were classified as larvae, 5 as juveniles and 22 as adults.
420 Sample IDs, number of raw reads and further parameters are listed in Table 1.
421
422 The sequence data was quality-checked using FastQC (Andrews 2010). Opsin gene expression
423 was then quantified using Geneious software version 11.0.3 (Kearse et al. 2012). For each
424 sample we first mapped the reads against a general fish reference dataset comprising all visual
425 opsin genes from the Nile tilapia, *Oreochromis niloticus* and the zebrafish, *Danio rerio*, with
426 the Medium-sensitivity settings in Geneious. This enabled us to identify cone and rod opsin
427 specific reads. If present, paralogous genes were subsequently disentangled following the
428 methods in Musilova et al. 2019a and de Busserolles et al. 2017. Briefly, we created species-
429 specific references of the expressed opsin genes and their several copies (Musilova et al. 2019a)
430 and re-mapped the transcriptome reads with Medium-Low sensitivity to obtain copy-specific
431 expression levels. If multiple opsin genes were found to be expressed, we report their
432 proportional expression in relation to the total opsin gene expression (Fig. 1). We used the same
433 pipeline to quantify expression of phototransduction cascade genes in five focal deep-sea
434 species (Fig. 2, Tables S1).
435
436 To check for key amino-acid substitutions in *RH1* and *RH2* and potential shifts in its
437 absorbance, we first translated the opsin coding sequences into amino acid sequences, and then
438 aligned them with the bovine *RH1* (GenBank Acc.No: M12689). We have specifically focused
439 on the positions identified as key-tuning sites in Yokoyama (2008) and Musilova et al. (2019a).

bioRxiv preprint doi: https://doi.org/10.1101/2020.05.25.114991; this version posted June 7, 2021. The copyright holder for this preprint (which was not certified by peer review) is the author/funder, who has granted bioRxiv a license to display the preprint in perpetuity. It is made available under aCC-BY-ND 4.0 International license.

For details, see Tables 2 and 3. Unfortunately, we were not able to estimate the exact sensitivity shift in *C. warmingii* as only four of the amino acids that were substituted at the 15 key-tuning amino acid sites corresponded with previously tested cases (Yokoyama, 2008, Musilova et al. 2019a). Out of the three copies, *RH1-2* has three out of four longer-shifting amino acid variants in these four sites and we assume is therefore red-shifted. *RH1-1* is most likely sensitive to 488 nm, and *RH1-3*, being the shortest, to 468nm.

In order to properly estimate the λ_{max} , we have further checked the samples for expression of the *Cyp27c1* gene, the factor assuming conversion of the A1 retinal to A2. Expression of *Cyp27c1* would assume that opsin protein bounds to the A2 instead of A1, which would cause a maximum shift of ca 25-30 nm (Enright et al. 2015). The expression of this gene has not been detected suggesting only A1 retinal in the studied species of the deep-sea fishes (Table S2).

A dataset containing *RH1* opsin gene sequences from our transcriptomes, and additional *RH1*s obtained from GenBank (link to NCBI) were aligned using the MAFFT (Katoh et al. 2009) plugin as implemented in Geneious and a phylogenetic tree was subsequently reconstructed using MrBayes v3.2.1 (Ronquist & Huelsenbeck 2003) (Fig. 2). Trees were produced using the Markov chain Monte Carlo analysis which ran for 1 million generations. Trees were sampled every 100 generations, and the printing frequency was 1000, discarding the first 25% of trees as burn-in. The evolutionary model chosen was GTR model with gamma-distributed rate variation across sites and a proportion of invariable sites. Posterior probabilities (PP) were calculated to evaluate statistical confidence at each node. We used the same approach with an *RH2*-specific reference dataset to reconstruct the phylogenetic relationship between the transcriptome-derived deep-sea *RH2* genes (Fig. 3).

Acknowledgements:

We would like to express our thanks to both scientific and technical crew of the Walther Herwig III research cruises in 2014 and 2017. In addition, we thank Tina Blancke for help with the sample management, and Veronika Truhlářová for technical support and lab management. NL and ZM were supported by the Swiss National Science Foundation (PROMYS - 166550) , ZM by the PRIMUS Research Programme (Charles University), the Czech Science Foundation (21-31712S) and the Basler Stiftung fuer Experimentelle Zoologie, and FC by an Australian Research Council (ARC) DECRA Fellowship (DE200100620).

bioRxiv preprint doi: https://doi.org/10.1101/2020.05.25.114991; this version posted June 7, 2021. The copyright holder for this preprint (which was not certified by peer review) is the author/funder, who has granted bioRxiv a license to display the preprint in perpetuity. It is made available under aCC-BY-ND 4.0 International license.

474 **References**:

475

476 **Andrews, S.** FastQC: a quality control tool for high throughput sequence data. 2010 (2017).

477 **Baylor, D. A.** Photoreceptor signals and vision. Proctor lecture. *Investigative ophthalmology*
478 *& visual science 28.1* (1987)

479 **Betancur-R, R., et al.** Phylogenetic classification of bony fishes. *BMC evolutionary biology*,
480 17(1), 162 (2017).

481 **Biagioni, L. M., Hunt, D. M. & Collin, S. P.** Morphological characterization and topographic
482 analysis of multiple photoreceptor types in the retinae of mesopelagic hatchetfishes with
483 tubular eyes. *Frontiers in Ecology and Evolution*, 4, 25 (2016).

484 **Britt, L. L., Loew, E. R. & McFarland, W. N.** Visual pigments in the early life stages of
485 Pacific northwest marine fishes. *Journal of Experimental Biology* 204.14 (2001).

486 **Bowmaker, J. K., Hunt, D. M., & Jeffery, G.** Eel visual pigments revisited: The fate of retinal
487 cones during metamorphosis. *Visual neuroscience*, 25(3), 249 (2008).

488 **Bozzano, A., Pankhurst, P. M. & Sabatés, A.** Early development of eye and retina in
489 lanternfish larvae. *Visual neuroscience*, 24(3), 423-436 (2007).

490 **Byun, J. H., et al.** Gene expression patterns of novel visual and non-visual opsin families in
491 immature and mature Japanese eel males. *PeerJ*, 8, e8326 (2020).

492 **Carleton, K. L. & Kocher, T. D.** Cone opsin genes of African cichlid fishes: tuning spectral
493 sensitivity by differential gene expression. *Molecular biology and evolution* 18.8 (2001)

494 **Carleton, K. L., Dalton, B. E., Escobar-Camacho, D. & Nandamuri, S. P.** Proximate and
495 ultimate causes of variable visual sensitivities: insights from cichlid fish radiations. *Genesis*,
496 54(6), 299-325 (2016).

497 **Carleton, K. L., Escobar-Camacho, D., Stieb, S. M., Cortesi, F. & Marshall, N. J.** Seeing
498 the rainbow: mechanisms underlying spectral sensitivity in teleost fishes. *Journal of*
499 *Experimental Biology*, 223(8) (2020).

500 **Collin, S. P., Hoskins, R. V. & Partridge, J. C.** Seven Retinal Specializations in the Tubular
501 Eye of the Scopelarchus michaelsarsi: A Case Study in Visual Optimization. *Brain, Behavior*
502 *and Evolution*, 1998(09), 291–314 (1998).

503 **Collin, S. P. & Marshall, N. J.** Sensory Processing in Aquatic Environments. Springer-Verlag
504 New York (2003).

505 **Cortesi, F., et al.** Ancestral duplications and highly dynamic opsin gene evolution in
506 percomorph fishes. *Proceedings of the National Academy of Sciences* 112.5 (2015).

bioRxiv preprint doi: https://doi.org/10.1101/2020.05.25.114991; this version posted June 7, 2021. The copyright holder for this preprint (which was not certified by peer review) is the author/funder, who has granted bioRxiv a license to display the preprint in perpetuity. It is made available under aCC-BY-ND 4.0 International license.

Cortesi, F., et al. From crypsis to mimicry: changes in colour and the configuration of the visual system during ontogenetic habitat transitions in a coral reef fish. *Journal of Experimental Biology*, 219(16), 2545-2558 (2016).

Cortesi, F., et al. Visual system diversity in coral reef fishes. *Seminars in Cell & Developmental Biology*. Academic Press (2020).

Dalton, B. E., Lu, J., Leips, J., Cronin, T. W. & Carleton, K. L. Variable light environments induce plastic spectral tuning by regional opsin coexpression in the African cichlid fish, *Metriaclima zebra*. *Molecular ecology* 24,16 (2015).

de Busserolles, F., et al. Pushing the limits of photoreception in twilight conditions: The rod-like cone retina of the deep-sea pearlsides. *Science advances*, 3(11), eaao4709 (2017).

de Busserolles, F., Fogg, L., Cortesi, F. & Marshall, J. The exceptional diversity of visual adaptations in deep-sea teleost fishes. *Seminars in Cell & Developmental Biology*. Academic Press (2020).

Dalton, B. E., Loew, E. R., Cronin, T. W. & Carleton, K. L. Spectral tuning by opsin coexpression in retinal regions that view different parts of the visual field. *Proceedings of the Royal Society B: Biological Sciences* 281,1797 (2014).

Denton, E. J. Light and vision at depths greater than 200 metres. Light and life in the sea (1990): 127-148.

Denton, E. J., Herring, P. J., Widder, E. A. Latz, M. F. & Case, J. F. The roles of filters in the photophores of oceanic animals and their relation to vision in the oceanic environment. *Proceedings of the Royal Society of London. Series B. Biological Sciences* 225, 1238 (1985).

Douglas, R. H., Hunt, D. M. & Bowmaker, J. K. Spectral sensitivity tuning in the deep-sea. In Sensory Processing in Aquatic Environments (pp. 323-342). Springer, New York, NY (2003).

Douglas, R. H., Partridge, J. C. & Marshall, N. J. The visual systems of deep-sea fish. I. Optics, tapeta, visual and lenticular pigmentation. *Prog. Ret. Eye Res*, 17(4), 597-636 (1998).

Douglas, R. H., Genner, M. J., Hudson, A. G., Partridge, J. C. & Wagner, H. J. Localisation and origin of the bacteriochlorophyll-derived photosensitizer in the retina of the deep-sea dragon fish *Malacosteus niger*. *Scientific reports*, 6, 39395 (2016).

Downes, G. B. & Gautam, N. The G protein subunit gene families. *Genomics*, 62(3), pp.544-552 (1999).

Enright, J. M., et al. Cyp27c1 red-shifts the spectral sensitivity of photoreceptors by converting vitamin A1 into A2. *Current Biology*, 25(23), 3048-3057 (2015).

bioRxiv preprint doi: https://doi.org/10.1101/2020.05.25.114991; this version posted June 7, 2021. The copyright holder for this preprint (which was not certified by peer review) is the author/funder, who has granted bioRxiv a license to display the preprint in perpetuity. It is made available under aCC-BY-ND 4.0 International license.

Hope, A. J., Partridge, J. C., Dulai, K. S. & Hunt, D. M. Mechanisms of wavelength tuning in the rod opsins of deep-sea fishes. *Proceedings of the Royal Society of London. Series B: Biological Sciences*, 264(1379), 155-163 (1997).

Huang, Z., Titus, T., Postlethwait, J. H., & Meng, F. Eye Degeneration and Loss of otx5b Expression in the Cavefish *Sinocyclocheilus tileihornes*. *Journal of molecular evolution* 87.7 (2019).

Hunt, D. M., Dulai, K. S., Partridge, J. C., Cottrill, P. & Bowmaker, J. K. The molecular basis for spectral tuning of rod visual pigments in deep-sea fish. *Journal of Experimental Biology*, 204(19), 3333-3344 (2001).

Hunt, D. M., Fitzgibbon, J., Slobodyanyuk, S. J., Bowmaker, J. K. & Dulai, K. S. Molecular evolution of the cottoid fish endemic to Lake Baikal deduced from nuclear DNA evidence. *Molecular Phylogenetics and Evolution*, 8(3), 415-422 (1997).

Hunt, D. M., Hankins, M.W., Collin, S.P. & Marshall, N.J. Evolution of visual and non-visual pigments (Vol. 4). Boston, MA: Springer (2014).

Katoh, K., Asimenos, G. & Toh, H. Multiple alignment of DNA sequences with MAFFT. In Bioinformatics for DNA sequence analysis (pp. 39-64). Humana Press (2009).

Kawamura, S. & Tachibanaki, S. Explaining the functional differences of rods versus cones. *Wiley Interdisciplinary Reviews: Membrane Transport and Signaling* 1.5 (2012)

Kearse, M., et al. Geneious Basic: an integrated and extendable desktop software platform for the organization and analysis of sequence data. Bioinformatics, 28(12), 1647-1649 (2012).

La Vail, M. M., Rapaport, D. H. & Rakic, P. Cytogenesis in the monkey retina. *J. Comp. Neurol.* 309, 86-114. doi:10.1002/cne.903090107 (1991).

Lamb, T. D. Evolution of phototransduction, vertebrate photoreceptors and retina. *Progress in retinal and eye research*, 36, 52-119 (2013).

Lamb, T. D. Evolution of the genes mediating phototransduction in rod and cone photoreceptors. *Progress in Retinal and Eye Research*, p.100823 (2019).

Larhammar, D, Nordström K & Larsson, T. A. Evolution of vertebrate rod and cone phototransduction genes. *Philosophical Transactions of the Royal Society B: Biological Sciences*, 364(1531), pp.2867-2880 (2009).

Liu, D.. et al. The cone opsin repertoire of osteoglossomorph fishes: gene loss in mormyrid electric fish and a long wavelength-sensitive cone opsin that survived 3R. *Molecular biology and evolution* 36.3 (2019).

Lythgoe, J.N. Visual pigments and under- water vision. In: Light as an Ecological Factor (Rackham, O., ed.). Oxford: Blackwell (1966).

bioRxiv preprint doi: https://doi.org/10.1101/2020.05.25.114991; this version posted June 7, 2021. The copyright holder for this preprint (which was not certified by peer review) is the author/funder, who has granted bioRxiv a license to display the preprint in perpetuity. It is made available under aCC-BY-ND 4.0 International license.

Luehrmann, M. et al. Cardinalfishes (Apogonidae) show visual system adaptations typical of nocturnally and diurnally active fish. *Molecular ecology* 28.12 (2019).

Luo, DG., et al. "Apo-Opsin and Its Dark Constitutive Activity across Retinal Cone Subtypes." *Current Biology* 30.24 (2020)

Ma, J. X., et al. A visual pigment expressed in both rod and cone photoreceptors. *Neuron*, 32(3), 451-461 (2001).

Mariani, A. P. Photoreceptors of the larval tiger salamander retina. *Proceedings of the Royal society of London. Series B. Biological sciences* 227.1249 (1986)

Mears, A. J., et al. Nrl is required for rod photoreceptor development. *Nature genetics*, 29(4), 447-452 (2001).

Moser, H. G. & Smith, P. E. Larval fish assemblages and oceanic boundaries. *Bull. Mar. Sci*, 53(2), 283-289 (1993).

Munk, O. Changes in the visual cell layer of the duplex retina during growth of the eye of a deep-sea teleost, *Gempylus serpens* Cuvier, 1829. *Acta Zoologica*, 71(2), 89-95 (1990).

Musilova, Z., et al. Vision using multiple distinct rod opsins in deep-sea fishes. *Science*, 364(6440), 588-592 (2019).

Musilova, Z., et al. Evolution of the visual sensory system in cichlid fishes from crater lake Barombi Mbo in Cameroon. *Molecular Ecology*, (August), 5010–5031 (2019).

Musilova, Z., Salzburger, W., Cortesi, F. The Visual Opsin Gene Repertoires of Teleost Fishes: Evolution, Ecology and Function. Annual Review of Cell and Developmental Biology (in press)

Musilova, Z., & Cortesi, F. Multiple ancestral and a plethora of recent gene duplications during the evolution of the green sensitive opsin genes (RH2) in teleost fishes. bioRxiv (2021).

Partridge, J. C., Shand, J., Archer, S. N., Lythgoe, J. N., & van Groningen-Luyben, W. A. H. M. Interspecific variation in the visual pigments of deep-sea fishes. *Journal of Comparative Physiology A*, 164(4), 513-529 (1989).

Pointer, M. A., Carvalho, L. S., Cowing, J. A., Bowmaker, J. K. & Hunt, D. M. The visual pigments of a deep-sea teleost, the pearl eye *Scopelarchus analis*. *Journal of Experimental Biology*, 210(16), 2829-2835 (2007).

Raymond, P. A. Development and morphological organization of photoreceptors. In Neurobiology and Clinical Aspects of the Outer Retina (pp. 1-23). Springer, Dordrecht (1995).

Reif, W. E. Functions of scales and photophores in mesopelagic luminescent sharks. *Acta Zoologica*, 66(2), 111-118 (1985).

bioRxiv preprint doi: https://doi.org/10.1101/2020.05.25.114991; this version posted June 7, 2021. The copyright holder for this preprint (which was not certified by peer review) is the author/funder, who has granted bioRxiv a license to display the preprint in perpetuity. It is made available under aCC-BY-ND 4.0 International license.

Ronquist, F., et al. MrBayes 3.2: efficient Bayesian phylogenetic inference and model choice across a large model space. *Systematic biology*, 61(3), 539-542 (2012).

Sassa, C. & Hirota, Y. Seasonal occurrence of mesopelagic fish larvae on the onshore side of the Kuroshio off southern Japan. *Deep Sea Research Part I: Oceanographic Research Papers*, 81, 49-61 (2013).

Savelli, I., Flamarique, I. N., Iwanicki, T. & Taylor, J. S. Parallel opsin switches in multiple cone types of the starry flounder retina: tuning visual pigment composition for a demersal life style. *Scientific reports* 8, no. 1 (2018).

Schott, R. K., Bhattacharyya, N. & Chang, B. S. Evolutionary signatures of photoreceptor transmutation in geckos reveal potential adaptation and convergence with snakes. *Evolution*, 73(9), 1958-1971 (2019).

Schott, R. K., et al. Evolutionary transformation of rod photoreceptors in the all-cone retina of a diurnal garter snake. *Proceedings of the National Academy of Sciences*, 113(2), 356-361 (2016).

Sernagor, E., Eglen, S., Harris, B. & Wong, R. (Eds.). Retinal development. Cambridge University Press (2006).

Shen, Y. C. & Raymond, P. A. Zebrafish cone-rod (crx) homeobox gene promotes retinogenesis. *Developmental biology*, 269(1), 237-251 (2004).

Simoes, B. F., et al. Multiple rod–cone and cone–rod photoreceptor transmutations in snakes: evidence from visual opsin gene expression. *Proceedings of the Royal Society B: Biological Sciences*, 283(1823), 20152624 (2016).

Stieb, S. M., et al. A detailed investigation of the visual system and visual ecology of the Barrier Reef anemonefish, *Amphiprion akindynos*. *Scientific reports* 9.1 (2019).

Sugawara, T., et al. Parallelism of amino acid changes at the RH1 affecting spectral sensitivity among deep-water cichlids from Lakes Tanganyika and Malawi. *Proceedings of the National Academy of Sciences*, 102(15), 5448-5453 (2005).

Tettamanti, V., de Busserolles, F., Lecchini, D., Marshall, N.J. & Cortesi, F. Visual system development of the spotted unicornfish, *Naso brevirostris* (Acanthuridae). Journal of Experimental Biology, 222(24) (2019).

Torres-Dowdall, J., et al. Rapid and parallel adaptive evolution of the visual system of Neotropical Midas cichlid fishes. *Molecular biology and evolution* 34.10 (2017).

Turner, J. R., White, E. M., Collins, M. A., Partridge, J. C. & Douglas, R. H. Vision in lanternfish (Myctophidae): adaptations for viewing bioluminescence in the deep-sea." *Deep Sea Research Part I: Oceanographic Research Papers* 56, 6 (2009).

bioRxiv preprint doi: https://doi.org/10.1101/2020.05.25.114991; this version posted June 7, 2021. The copyright holder for this preprint (which was not certified by peer review) is the author/funder, who has granted bioRxiv a license to display the preprint in perpetuity. It is made available under aCC-BY-ND 4.0 International license.

641 **Underwood, G.** Some suggestions concerning vertebrate visual cells. *Vision research*, 8(4),
642 483-488 (1968).
643 **Valen, R., et al.** The two-step development of a duplex retina involves distinct events of cone
644 and rod neurogenesis and differentiation. *Developmental biology*, 416(2), 389-401 (2016).
645 **Wagner, H. J., Partridge, J. C. & Douglas, R. H.** Observations on the retina and 'optical
646 fold'of a mesopelagic sabretooth fish, *Evermanella balbo*. *Cell and Tissue Research*, 378(3),
647 411-425 (2019).
648 **Yokoyama, S.** Evolution of dim-light and color vision pigments. *Annu. Rev. Genomics Hum.*
649 *Genet.*, 9, 259-282 (2008).
650 **Yokoyama, S. & Jia, H.** Origin and adaptation of green-sensitive (RH2) pigments in
651 vertebrates. *FEBS Open Bio*, 10(5), 873-882 (2020).
652 **Zhang, H., et al.** Molecular cloning of fresh water and deep-sea rod opsin genes from Japanese
653 eel *Anguilla japonica* and expressional analyses during sexual maturation. *Febs Letters*,
654 469(1), 39-43 (2020).

bioRxiv preprint doi: https://doi.org/10.1101/2020.05.25.114991; this version posted June 7, 2021. The copyright holder for this preprint (which was not certified by peer review) is the author/funder, who has granted bioRxiv a license to display the preprint in perpetuity. It is made available under aCC-BY-ND 4.0 International license.

Table 1: Samples used in the study and results of the opsin gene expression in the eyes or retina

species	order	stage	code	size	date of collection	raw reads	reads after bacteria filtering	RH1	RH2	SWS1	SWS2	accession number
Anoplogaster cornuta	Trachichthyiformes	Larva	39016	4mm		36,373,372	36,125,630	<0.01	0.99		<0.01	
		Larva	39017	4mm		34,712,538	34,604,364	<0.01	0.99		<0.01	
		Larva	4_23	9mm		41,592,840	41,519,070	0.02	0.98		<0.01	
		Larva	4_22	11mm		75,109,270	74,990,214	0.11	0.89		<0.01	
		Larva	4_21	11-12 mm		28,945,804	28,869,552	0.22	0.78		<0.01	
		Larva	261s03	12mm		48,458,044	48,457,472	0.47	0.53		<0.01	
		Adult	56H6			11,658,040	11,635,610	1				
Ceratoscopelus warmingii	Myctophiformes	Adult	300s03	63mm		49,078,974	44,114,639	0.66^{RH1-1}				
								0.01^{RH1-2}				
								0.33^{RH1-3}				
		Adult	S1			8,796,786	8,789,961	0.94^{RH1-1}				
								0.02^{RH1-2}				
								0.04^{RH1-3}				
		Adult	S2			8,655,248	8,649,342	0.93^{RH1-1}				
								0.02^{RH1-2}				
								0.05^{RH1-3}				
		Adult	S3			7,904,714	7,899,617	0.94^{RH1-1}				
								0.01^{RH1-2}				
								0.05^{RH1-3}				
Chauliodus sloani	Stomiiformes	Larva	67I2_2	11mm		34,445,252	34,371,394	0.01	0.99			
		Larva	67I1	17mm		20,701,686	20,683,764	<0.01	0.99			
		Juvenile	109B6	20mm		24,854,866	24,835,646	1				
Chauliodus danae	Stomiiformes	Juvenile	109C7	24mm		32,865,334	32,834,300	1				
		Juvenile	109A2	20mm		25,389,318	25,344,182	1				
		Juvenile	109D7			18,540,248	18,533,484	1				
Coccorella atlantica	Aulopiformes	Larva	109G8			26,376,620	26,359,060	0.01	0.99^{RH2-1}			
		Adult	56C7			36,794,070	36,790,854	0.69	0.31^{RH2-2}			
		Adult	297_7	68mm		43,948,534	40,511,279	0.96	0.04^{RH2-3}			
Grammatostomias flagellibarba	Stomiiformes	Adult	56H8			9,775,520	9,742,864	1				
Gyrinomimus myersi	Beryciformes	Larva	S25			19,270,096	19,122,986	<0.01	0.45^{RH2-1}	0.07	<0.01	
									0.13^{RH2-2}			
									0.08^{RH2-3}			
									0.11^{RH2-4}			
									0.15^{RH2-5}			
Howella brodiei	Pempheriformes	Adult	56D8			56,905,264	43,936,178	0.17^{RH1-1}				
								0.83^{RH1-2}				
		Adult	56D9			61,909,674	61,590,270	0.07^{RH1-1}				
								0.93^{RH1-2}				
Hygophum reinhardtii	Myctophiformes	Larva	67I2_1	5mm		17,222,626	17,122,880		0.26^{RH2-1}			
									0.68^{RH2-2}			
									0.06^{RH2-3}			
Idiacanthus fasciola	Stomiiformes	Larva	71C2			23,382,468	23,379,360		1			
		Larva	67D2			6,647,384	6,623,496		1			
		Larva	71C1			23,632,774	23,497,715		1			
		Larva	67I7	25mm		25,713,960	25,701,768		1			
		Larva	71B9			43,695,620	43,633,424		1			
		Larva	67B8			28,333,642	28,313,024		1			
		Larva	109A1	41mm		27,834,274	27,818,750		1			
		Adult	228s01			21,704,528	21,622,274	1				
		Adult	67F8			15,744,604	15,739,004	1				
		Adult	67B6			11,368,044	15,439,954	1				
Melamphaes sp.	Beryciformes	Juvenile	4_26			38,583,370	38,534,507	1				
		Juvenile	4_28			35,489,970	35,431,421	1				
Melanolagus bericoides	Argentiniformes	Larva	71H3			26,219,646	26,210,402		1			
Pteraclis aesticola	Scombriformes	Larva	109H4			19,918,922	19,870,484	0.22	0.78			
Pollichthys mauli	Stomiiformes	Adult	109I2			55,767,498	54,875,747	1				
		Adult	109I3			68,655,686	67,082,709	1				
Scombrolabrax heterolepis	Scombriformes	Adult	,56E3			65,770,014	5,527,135	0.98	0.02			
		Adult	,56E4			60,643,652	60,472,479	0.93	0.07			
Scopelarchus guentheri	Aulopifoformes	Larva	109H1			37,542,802	37,416,486		0.96^{RH2_larval}			
									0.04^{RH2_2nd_larval}			
Scopelarchus michaelsarsi	Aulopifoformes	Larva	109B9	21mm		9,971,250	9,919,148		1^{RH2_larval}			
		Larva	71B7			43,695,620	43,682,534	<0.01^{RH1a}	0.96^{RH2_larval}			
								<0.01^{RH1b}	0.03^{RH2_2nd_larval}			
		Adult	272_10	66mm		45,565,202	43,729,338	0.80^{RH1a}	0.10^{RH2_adult}			
								0.10^{RH1b}				
Scopelogadus mizolepis	Beryciformes	Adult	,57E2			5,160,876	5,160,876	1				
		Adult	300s01			15,448,240	15,420,650	1				
Scopelosaurus hoedti	Aulopiformes	Adult	297_9	69mm		43,948,534	42,248,053	0.98	0.02			
Vinciguerria poweriae	Stomiiformes	Larva	109H2			25,863,628	25,755,100		1			
		Larva	109C8	16mm		22,914,004	22,858,398		1			

bioRxiv preprint doi: https://doi.org/10.1101/2020.05.25.114991; this version posted June 7, 2021. The copyright holder for this preprint (which was not certified by peer review) is the author/funder, who has granted bioRxiv a license to display the preprint in perpetuity. It is made available under aCC-BY-ND 4.0 International license.

Table 2: key-tuning amino acid sites in the cone opsin RH2 gene

species	order	83	122	207	255	292	lmax	ref.
Bovine RH1		D	E	M	I	A	500 nm	41
Ancestral teleost		D	Q	M	I	A	488 nm	42
Melanolagus bericoides	Argentiniformes	G	Q	.	V	.		
Coccorella atlantica adult	Aulopiformes	G	Q	.	.	.		
Coccorella atlantica larval	Aulopiformes	G	Q	.	V	.		
Scopelarchus michaelsarsi adult	Aulopiformes	?	Q	I	C	T		
Scopelarchus guentheri larval	Aulopiformes	G	Q	.	V	.		
Scopelarchus michaelsarsi larval	Aulopiformes	G	Q	.	V	.	505 nm	21
Scopelarchus guentheri 2nd larval	Aulopiformes	G	Q	.	C	.		
Scopelarchus michaelsarsi 2nd larval	Aulopiformes	G	Q	.	C	.		
Scopelosaurus hoedti	Aulopiformes	G	Q	.	.	.		
Gyrinomimus myersi RH2-1	Beryciformes	G	Q	.	F	.		
Gyrinomimus myersi RH2-2	Beryciformes	G	Q	L	F	.		
Gyrinomimus myersi RH2-3	Beryciformes	G	Q	L	F	.		
Gyrinomimus myersi RH2-4	Beryciformes	G	Q	L	F	.		
Gyrinomimus myersi RH2-5	Beryciformes	G	Q	L	F	.		
Lepisosteus platyrhincus	Lepisosteiformes	G	.	.	.	.		
Hygophum reinhardtii RH2-1	Myctophiformes	G	Q	.	V	.		
Hygophum reinhardtii RH2-2	Myctophiformes	G	Q	.	V	.		
Hygophum reinhardtii RH2-3	Myctophiformes	G	Q	.	V	.		
Lepidopus fitchi RH2-1	Scombriformes	G	.	.	V	.	496 nm	42
Lepidopus fitchi RH2-2	Scombriformes	G	Q	.	V	.		
Lepidopus fitchi RH2-3	Scombriformes	G	Q	.	V	.	506 nm	42
Lepidopus fitchi RH2-4	Scombriformes	G	Q	.	V	.		
Pteraclis aesticola	Scombriformes	G	Q	L	.	.		
Scombrolabrax heterolepis	Scombriformes	G	Q	.	.	.		
Aristostomias scintillans	Stomiiformes	G	Q	L	V	.	468 nm	42
Chauliodus sp.	Stomiiformes	G	Q	.	F	.		
Grammastomias flagellibarba	Stomiiformes	G	Q	.	.	.		
Idiacanthus fasciola	Stomiiformes	G	Q	.	V	.		
Vinciguerria poweriae	Stomiiformes	G	Q	.	F	.		
Anoplogaster cornuta	Trachichthyiformes	G	Q	.	.	.		

bioRxiv preprint doi: https://doi.org/10.1101/2020.05.25.114991; this version posted June 7, 2021. The copyright holder for this preprint (which was not certified by peer review) is the author/funder, who has granted bioRxiv a license to display the preprint in perpetuity. It is made available under aCC-BY-ND 4.0 International license.

Table 3: key-tuning amino acid sites in the rhodopsin RH1 gene

Species	Order	83	90	96	102	111	113	118	122	124	132	164	183	188	194	195	207	208	211	214	253	261	265	269	289	292	295	299	300	317	lmax	ref.
bovine RH1		D	G	Y	Y	N	E	T	E	A	A	A	M	G	P	H	M	F	H	I	M	F	W	A	T	A	A	A	V	M	500 nm	41
ancestral teleost RH1		D	G	Y	Y		E	T	E	A	A	A	M		L	N	M	F	H	I	M	F	W	A	T	A	A	A	L	M		16
Bathysaurus ferox	Aulopiformes	N	.	.	.	.	.	.	.	S	.	.	.	.	R	A	.	.	.	.	.	.	.	.	.	S	.	T	L	.	481 nm	50
Bathysaurus mollis	Aulopiformes	N	.	.	.	.	.	.	.	S	.	.	.	.	R	A	.	.	.	.	.	.	.	T	.	S	.	T	L	.	479 nm	50
Coccorella atlantica	Aulopiformes	N	.	.	.	S	.	.	M	.	.	.	.	.	R	A	.	.	.	C	.	.	.	.	.	.	S	.	I	.	480 nm‡	64
Scopelarchus spp. RH1-1	Aulopiformes	N	.	.	.	.	.	.	.	.	.	.	.	.	R	A	.	.	.	C	.	.	.	.	.	S	S	S	I	.	486 nm	21
Scopelarchus spp. RH1-2	Aulopiformes	N	.	.	.	.	.	.	.	S	.	.	.	.	L	K	.	.	.	V	.	.	.	.	.	S	.	.	L	.	479 nm	21
Scopelosaurus hoedti	Aulopiformes	.	.	.	.	.	.	.	.	.	.	.	.	.	R	A	.	.	.	.	.	.	.	.	.	S	S	S	I	.		
Gyrinomimus myersi	Beryciformes	N	.	.	.	.	.	.	.	.	.	.	.	.	R	A	.	.	.	.	.	.	.	.	.	S	.	.	I	.		
Melamphaes sp.	Beryciformes	.	.	.	.	.	.	.	Q	.	S	.	.	.	R	V	.	.	.	G	.	.	.	S	.	.	.	S	I	.		
Scopelogadus mizolepis	Beryciformes	.	.	.	.	.	.	.	Q	G	S	.	.	.	R	V	.	.	.	G	.	.	.	T	.	.	.	S	.	.	488 nm§	64
Lepisosteus oculatus	Lepisosteiformes	.	.	.	.	.	.	.	Q	S	.	.	.	.	L	K	.	.	.	L	.	Y	.	G	.	.	.	.	L	.		
Ceratoscopelus warmingii RH1-1	Myctophiformes	.	.	.	.	T	.	.	Q	.	S	.	.	.	R	A	.	.	.	G	.	.	.	.	.	.	.	S	I	.	?468 nm†	50
Ceratoscopelus warmingii RH1-2	Myctophiformes	.	.	W	.	I	.	.	I	T	.	.	.	.	R	A	.	.	.	V	.	Y	.	.	.	.	.	.	I	.	prob. 488 nm†	50
Ceratoscopelus warmingii RH1-3	Myctophiformes	.	.	.	.	A	.	.	Q	.	S	S	.	.	N	V	.	.	Y	G	.	.	.	.	.	S	.	.	I	.	?468 nm†	50
Hygophum reinhardtii	Myctophiformes	.	.	.	.	A	.	.	Q	.	.	.	.	.	R	A	.	.	.	G	.	.	.	.	.	.	.	.	I	.		
Howella brodiei RH1-1	Pempheriformes	N	.	.	.	.	.	.	.	G	.	.	.	.	R	A	.	.	.	.	.	.	.	.	G	S	S	S	I	.		
Howella brodiei RH1-2	Pempheriformes	N	.	.	.	.	.	.	Q	S	.	.	.	.	R	A	.	.	.	A	.	.	.	.	.	S	S	S	I	.		
Pteraclis aesticola	Scombriformes	.	.	.	.	.	.	.	Q	.	.	.	.	.	R	A	.	.	.	.	.	.	.	.	.	.	.	S	I	.		
Scombrolabrax heterolepis	Scombriformes	.	.	.	.	.	.	.	Q	.	.	.	.	.	R	A	.	.	.	.	.	.	.	S	.	S	.	S	I	.		
Chauliodus spp.	Stomiiformes	N	.	.	.	.	.	.	.	G	.	.	.	.	R	A	.	.	.	V	.	.	.	.	A	S	.	.	L	V	484 nm	50
Grammatostomias flagellibarba	Stomiiformes	N	.	.	.	.	.	.	.	.	.	.	.	.	R	A	.	.	.	V	.	.	.	.	.	S	.	.	L	.	480 - 487 nm	65
Idiacanthus fasciola	Stomiiformes	N	.	.	.	.	.	.	.	.	.	.	.	.	R	A	.	.	.	.	.	.	.	.	.	S	.	.	L	.	485 nm	50
Pollichthys mauli	Stomiiformes	N	.	.	.	.	.	.	.	.	.	.	.	.	R	A	.	.	.	.	.	.	.	.	.	S	.	.	L	.		
Anoplogaster cornuta	Trachichthyiformes	N	.	.	.	.	.	.	.	.	.	.	.	.	R	A	.	.	.	.	.	.	.	.	T	S	.	S	I	.	485 nm	50

† = two pigments reported without assignment to the gene; see also Figure 3

‡ = for *Evermannella balbo* ; sequence not available

§ = for *Scopelogadus beani* ; sequence not available